CERN-EP/83-23
7 February 1983

PRELIMINARY SEARCHES FOR HADRON JETS AND FOR LARGE TRANSVERSE MOMENTUM ELECTRONS AT THE SPS $\bar{p}p$ COLLIDER.

The UA2 Collaboration.

M. Banner[f], R. Battiston[*,£], Ph. Bloch[f], F. Bonaudi[b], K. Borer[a], M. Borghini[b], J.-C. Chollet[d], A.G. Clark[b], C. Conta[e], P. Darriulat[b], L. Di Lella[b], J. Dines-Hansen[c], P-A. Dorsaz[b], L. Fayard[d], M. Fraternali[e], D. Froidevaux[b], J-M. Gaillard[d], O. Gildemeister[b], V.G. Goggi[e], H. Grote[b], B. Hahn[a], H. Hänni[a], J.R. Hansen[b], P. Hansen[c], T. Himel[b], V. Hungerbühler[b], P. Jenni[b], O. Kofoed-Hansen[c], E. Lançon[f], M. Livan[b,e], S. Loucatos[f], B. Madsen[c]. P. Mani[a], B. Mansoulié[f], G.C. Mantovani[*], L. Mapelli[b], B. Merkel[d], M. Mermikides[b], R. Møllerud[c], B. Nilsson[c], C. Onions[b], G. Parrour[b,d], F. Pastore[b,e], H. Plothow-Besch[b,d], M. Polverel[f], J-P. Repellin[d], A. Rothenberg[b], A. Roussarie[f], G. Sauvage[d], J. Schacher[a], J-L. Siegrist[b], H.M. Steiner[†(b)], G. Stimpfl[b], F. Stocker[a], J. Teiger[f], V. Vercesi[e], A. Weidberg[b], H. Zaccone[f] and W. Zeller[a].

a) Laboratorium für Hochenergie physik, Universität Bern, Sidlerstrasse 5, Bern, Switzerland.

b) CERN, 1211 Geneva 23, Switzerland.

c) Niels Bohr Institute, Blegdamsvej 17, Copenhagen, Denmark.

d) Laboratoire de l'Accélérateur Linéaire, Université de Paris-Sud, Orsay, France.

e) Istituto di Fisica Nucleare, Università di Pavia and INFN, Sezione di Pavia, Via Bassi 6, Pavia, Italy.

f) Centre d'Etudes nucléaires de Saclay.

* Gruppo INFN del Dipartimento di Fisica dell'Università di Perugia (Italy)

† On leave from Lawrence Berkeley Laboratory, USA.

£ Also at Scuola Normale Superiore, Pisa, Italy.

Presented at the Third Topical Workshop
on proton-antiproton Collider Physics
Rome, January 12-14, 1983

ABSTRACT

We present a preliminary analysis of the UA2 data collected during the last Collider run (20 nb^{-1} integrated luminosity) with particular emphasis on large transverse momentum hadron jets and on electrons having the configuration expected from the decay of electroweak bosons. The data provide very strong evidence of two-jet dominance in events with large transverse energy in the central region.

Four electron candidates have been observed with a transverse momentum in excess of 20 GeV/c, which are associated with no other large transverse energy production within the UA2 acceptance. While this result is in all respects consistent with a $W \rightarrow e\nu$ hypothesis, more work is needed to ensure that the background is well understood and to further ascertain electron identification.

No electron pair was detected with an invariant mass in excess of 40 GeV/c^2.

1. INTRODUCTION

During the months of October and November 1982 the UA2 experiment took data at the SPS $\bar{p}p$ Collider [1] for an integrated luminosity of nearly 20 nb^{-1}, namely $\sim$ 250 times larger than in the earlier 1981 period of data collection [2,3] . Less than two months later the Rome Workshop provides an opportunity to present a preliminary analysis of a selected sample of the collected data, with particular emphasis on a search for electroweak bosons. The conjecture that such particles exist [4] has been the main incentive behind the construction of the SPS $\bar{p}p$ Collider and of its associated detectors. According to current expectations [5], and for an integrated luminosity of $\sim$ 20 nb^{-1}, the numbers of events in which an electroweak boson decays within the UA2 acceptance are respectively

$$\begin{aligned} &\sim 20 \quad \text{for} \quad (W^{\pm}, Z^{o}) \rightarrow \text{hadrons} \\ &\sim 4 \quad \text{for} \quad W^{\pm} \rightarrow e^{\pm}\nu \ , \ p_T^e > 15 \text{ GeV/c} \\ \text{and} \ &\sim \tfrac{1}{2} \quad \text{for} \quad Z^{o} \rightarrow e^{+}e^{-}. \end{aligned}$$

2. DETECTOR AND DATA TAKING : GENERAL DESCRIPTION

2.1 - DETECTOR.

The UA2 detector [2,3,6] was designed mainly with the aims to observe electroweak boson decays and to study final states containing large transverse momentum hadron jets : such phenomena are expected to result from the collisions at very short distance accessible to the SPS $\bar{p}p$ Collider, the only existing facility providing a sufficient centre of mass energy, $\sqrt{s}$ = 540 GeV. The expectation that the collision products relevant to the study of such processes populate mostly the central rapidity region led to restrict the detector coverage to $\sim$ 3.5 rapidity units, within which, for example, $\sim$ $^2/_3$ of Z^o decays are expected to occur. The cones corresponding to scattering angles $\theta < 20^o$, $\theta > 140^o$ are not covered by UA2 but are left open to house the detectors of experiment UA4 [7] designed to measure the elastic and total $\bar{p}p$ cross sections.

Despite their small branching fractions the leptonic decay modes of the electroweak bosons

$$\begin{aligned} &W^{\pm} \rightarrow l^{\pm}\nu \quad (\text{BR} \simeq 8\% \text{ per lepton type}) \\ \text{and} \ &Z^{o} \rightarrow l^{+}l^{-} \quad (\text{BR} \simeq 3\% \text{ per lepton type}) \end{aligned}$$

are supposed to be the least difficult to detect because of the very small expected background contamination. For this reason UA2 was designed to detect and identify electrons over its whole acceptance; electrons were preferred over muons because excellent energy resolutions can be achieved in compact calorimeters.

Hadron detection is also implemented over the whole UA2 acceptance but different approaches have been adopted in the central ($40 < \theta < 140^{o}$) and forward ($20 < \theta < 40^{o}$, $140 < \theta < 160^{o}$) regions. The central region is instrumented with a highly segmented hadron calorimeter having a cell configuration well suited to the observation of hadron jets independently of their mode of fragmentation. The forward regions, where important $W \to e\nu$ charge asymmetries are expected to occur, are equipped with two magnetic spectrometers, each consisting of a toroidal field magnet followed by nine drift chamber planes.

A set of cylindrical wire chambers densely packed around the beam in the collision region provide measurements of the position of the event vertex and of the directions of the charged particles produced in the collision. It is made of four proportional chambers with helicoidal cathode strips and of two drift chambers of 24 azimuthal cells each, with six drift wires per cell.

The measurement of a track pointing to an energy deposition localised in one of the electron calorimeter cells provides a powerful means of selecting electron candidates but it leaves a significant contamination of narrow π^{0}- charged hadron pairs (overlap background). This is strongly reduced by using preshower counters in front of the electron calorimeters to provide improved space resolution. The central preshower counter is a cylindrical proportional chamber with helicoidal cathode strips and the forward preshower counters are proportional tube planes. Each is preceded by a $\sim$ 1.5 radiation length thick converter.

In the central region a $\Delta \phi = 60^{o}$ azimuthal wedge was left open to house a large angle magnetic spectrometer [3] instrumented over a $\Delta \phi$. $\Delta \theta \simeq 30^{o} \times 70^{o}$ solid angle with drift chambers, scintillator hodoscopes and a lead-glass array. It has provided detailed information on inclusive particle production around 90^{o}. It is now in the process of being closed to lead to an azimuthally symmetric detector configuration better suited to the study of the topics of present interest (electroweak bosons and large transverse momentum jets).

The main detector parameters are listed in Table 1. Figures 1a and b show schematic views of the detector assembly.

2.2 - DATA TAKING

The data discussed in this report were recorded using triggers sensitive to events with large transverse energy in the central and forward calorimeters. They were of three types :

- The ΣE_{T} trigger required a total transverse energy (ΣE_{T}) measured in the central calorimeter (electron and hadron cells linearly added) in excess of $\sim$ 35 GeV,
- the W trigger required the presence of at least one quartet (2 × 2) of electron calorimeter cells (central or forward) in which the measured transverse energy exceeded $\sim$ 8 GeV,

TABLE 1

MAIN PARAMETERS OF THE UA2 DETECTOR

I. SOLID ANGLE COVERAGE

Central region. Electron-hadron calorimetry.
$\Delta y \simeq 2$, $\Delta\theta \simeq 100^{\circ}$, $\Delta\phi \simeq 300^{\circ}$

Forward-backward regions. Electron calorimetry and magnetic spectroscopy.
$\Delta y \simeq 1.5$, $\Delta\theta \simeq 35^{\circ}$, $\Delta\phi \simeq 82\%$ of 360°

Wedge region. Electron calorimetry and magnetic spectroscopy.
$\Delta y \simeq 1.3$, $\Delta\theta \simeq 68^{\circ}$, $\Delta\phi \simeq 28^{\circ}$

II. CENTRAL CALORIMETER

200 cells, each covering $\Delta\theta \times \Delta\phi = 10^{\circ} \times 15^{\circ}$.
Longitudinal segmentation
17 r.l. (lead-scintillator) + 2 × 2 abs. l. (iron-scintillator)
Electron calorimetry 26 × 3.5 mm lead plates
27 × 4 mm NE 104 scintillator plates
Hadron calorimetry (18 + 22) × 15 mm iron plates
(18 + 22) × 5 mm scintillator plates
(PMMA, 10% naphtalene, 1% PBD, 0.01% POPOP)
Light guides : 2 mm lucite, 80 mg/l BBQ
Phototubes : 7 per cell, XP2012 for electron calorimetry and XP2008 for hadron calorimetry

III. FORWARD DETECTORS

24 identical sectors each covering $\Delta\theta \times \Delta\phi = 17.5^{\circ} \times 25^{\circ}$
Field integral 0.38 Tm.
9 drift chambers per sector
- wire orientation with respect to field : -7°, 0°, $+7^{\circ}$.
- drift cell width ±5 cm
- field shaping wires every 5 mm
- total number of signal wires 2304.

preshower counter
- preconverter 1.4 r.l. lead + iron
- 4 tube planes (brass) 20 mm O.D., 0.3 mm thick.
- tube orientation with respect to field : 0°, 0°, 77°, 77°.

- anode 30 micron gold plated tungsten

forward calorimeters

- 10 cells per sector, each covering $\Delta\theta \times \Delta\phi \simeq 4^{o} \times 15^{o}$
- cell transverse sizes 27 × 33 to 27 × 60 cm^2
- longitudinal segmentation : 33 × (4 mm lead + 4 mm Altustipe 10105) + 8 × (4 mm lead + 4 mm Altustipe 10105) = 24 + 6 r.l.
- light guides and phototubes as in central calorimeter.

IV. VERTEX DETECTOR

- five proportional chambers with cathode strip read-out, one of which is located behind a 1.5 r.l. tungsten converter.

number of strips	480, 480, 528, 672 and 480.
number of wires	288, 384, 576, 864 and 576.
chamber radii	100, 124, 236, 315 and 355 mm.
chamber lengths	104, 110, 150, 178 and 80 cm.
wire pitch	2.2, 2.0, 2.6, 2.3 and 3.9 mm.
strip angle	tan $\alpha = \pm$ 0.9, 1.3, 1.0, 1.0, 1.0 .
half gap	4 mm
strip pitch	$\simeq$ 4 mm.

- two drift chambers of 24 azimuthal cells each, 6 sense wires/cell (charge division, multihit capability), sense wire lengths 1520 and 1785 mm
- 24 scintillator plates.

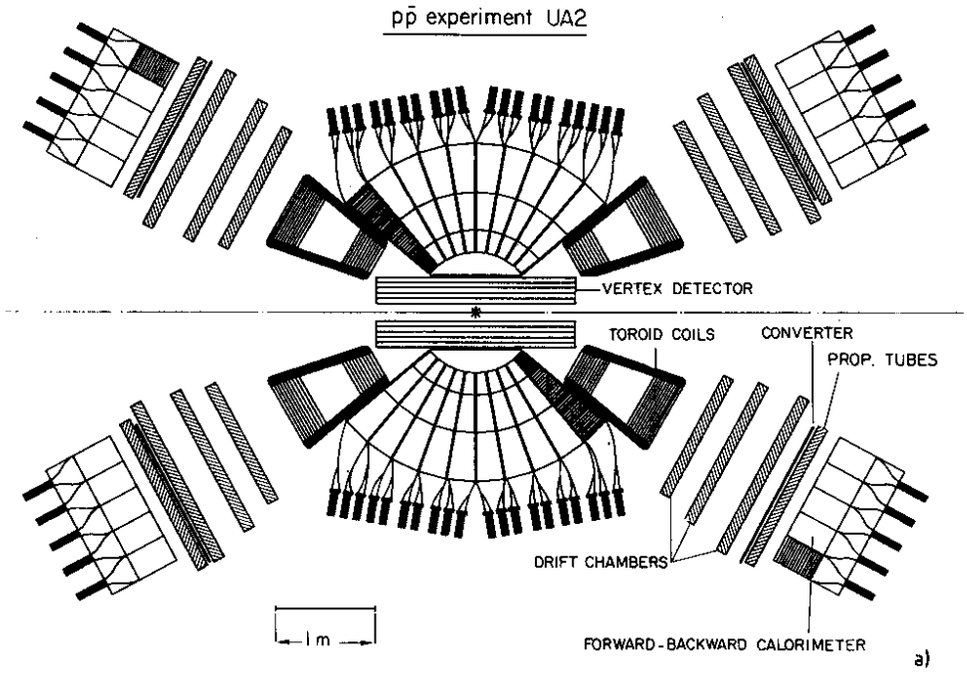

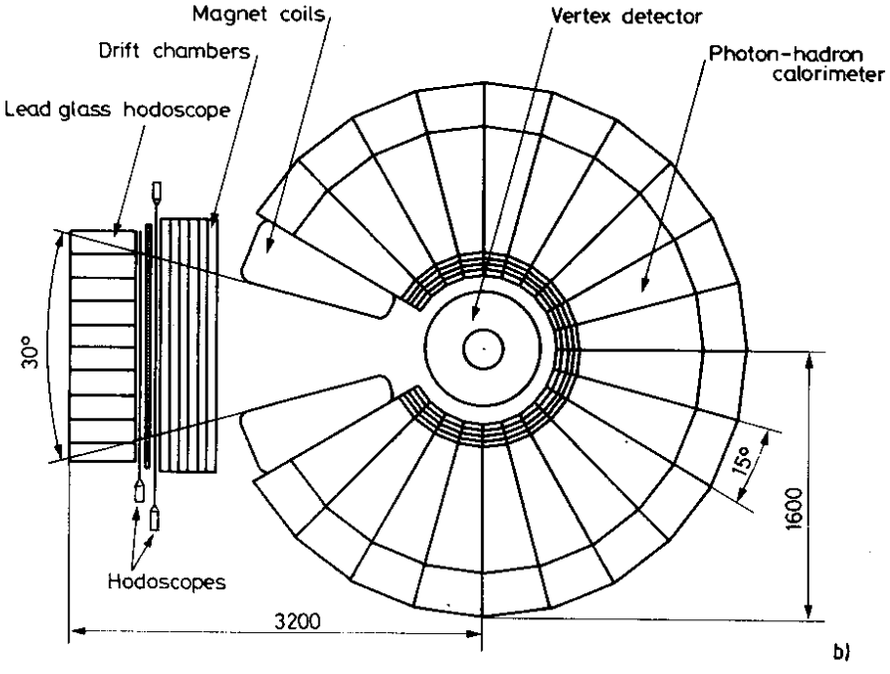

Figure 1.

Schematic detector assembly :

a) longitudinal cut along the beam,

b) transverse cut normal to the beam.

- the Z^0 trigger required the presence of two such quartets, each having a transverse energy in excess of $\sim$ 3.5 GeV, and azimuthally separated by $\Delta \phi > 60^\circ$.

In addition the ΣE_T and W triggers (but not the Z^0 trigger) required a coincidence with two signals obtained from scintillator arrays covering an angular range $0.47 < \theta < 2.84^\circ$ on both sides of the collision region. This additional condition is satisfied by nearly all non-diffractive collisions [7]. Early signals measured in these scintillator arrays were used to tag background events induced by beam halo particles interacting in the detector.

3. LARGE TRANSVERSE ENERGY HADRONS.

3.1 - THE CENTRAL CALORIMETER.

In the present Section we restrict the analysis to events which satisfy the ΣE_T trigger. The central calorimeter is the part of the UA2 detector which is most relevant to the present study. It is segmented into 200 cells, each covering 15° in ϕ and 10° in θ, and built in a tower structure pointing towards the centre of the interaction region. The cells (Figure 2) are segmented longitudinally into a 17 radiation length thick electromagnetic compartment (lead-scintillator) followed by two hadronic compartments (iron-scintillator) of two absorption lengths each. The light from each compartment is collected by two BBQ-doped light guide plates on opposite sides of the cell.

All calorimeters, including the forward modules, have been calibrated in a 10 GeV/c beam from the CERN PS using incident electrons and muons. The calibration has since be tracked with a Xe light flasher system. In addition, the response of the electromagnetic compartments is checked regularly by accurately positioning a Co^{60} source in front of each cell and measuring the direct current from each photomultiplier. The systematic uncertainty in the energy calibration for the data discussed here is less than ±2% for the electromagnetic calorimeter and less than ±3% for the hadronic one.

The response of the calorimeter to electrons, single hadrons and multi-hadrons (produced in a target located in front of the calorimeter) has been measured at the CERN PS and SPS machines using beams from 1 to 70 GeV. In particular we have studied the longitudinal and transverse shower development and the effect of particles impinging near the cell boundaries.

The energy resolution for electrons is measured to be $\sigma_E/E = 0.14 / \sqrt{E}$ (E in GeV). In the case of hadrons, σ_E/E varies from 32% at 1 GeV to 11% at 70 GeV, approximately like $E^{-1/4}$. The resolution for multi-hadron systems of more than 20 GeV is similar to that of single hadrons.

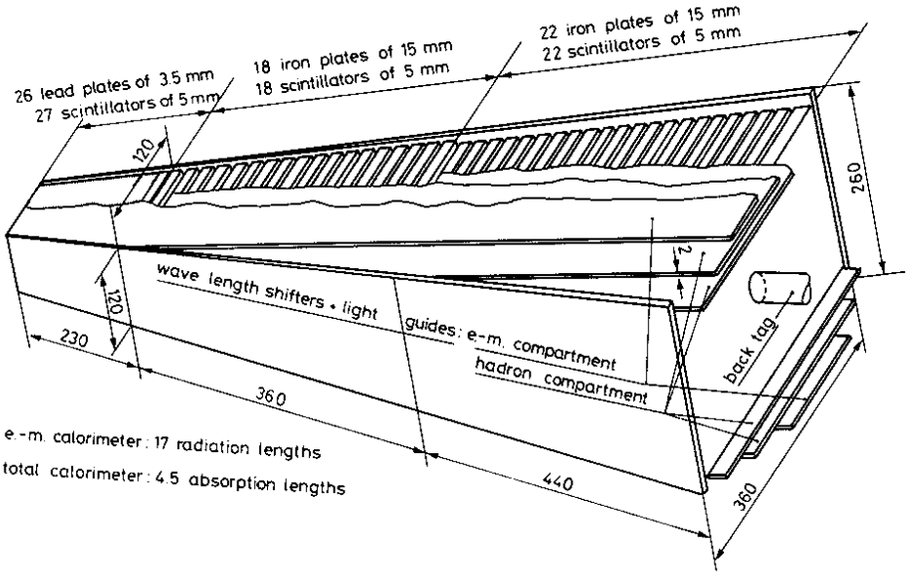

Figure 2. Exploded view of a central calorimeter cell.

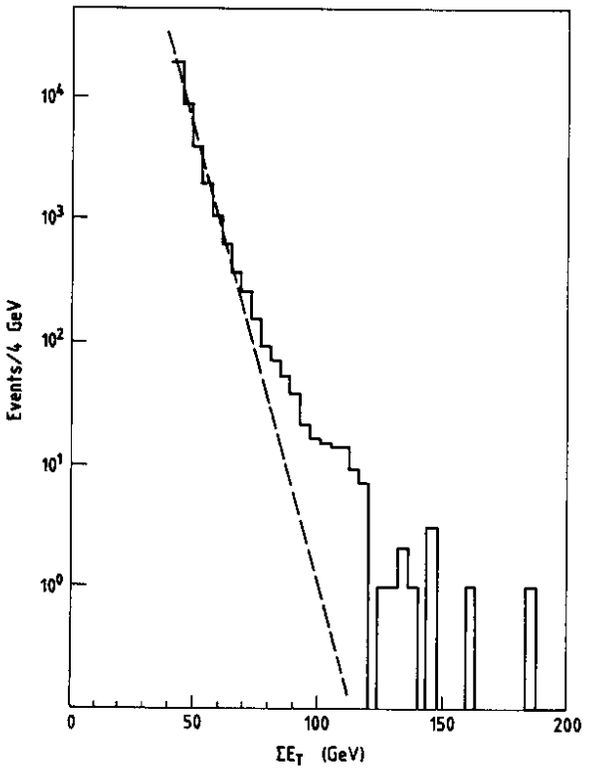

Figure 3.
Observed (uncorrected) ΣE_T distribution in the central calorimeter. The line is an exponential eye-fit to the data at low ΣE_T.

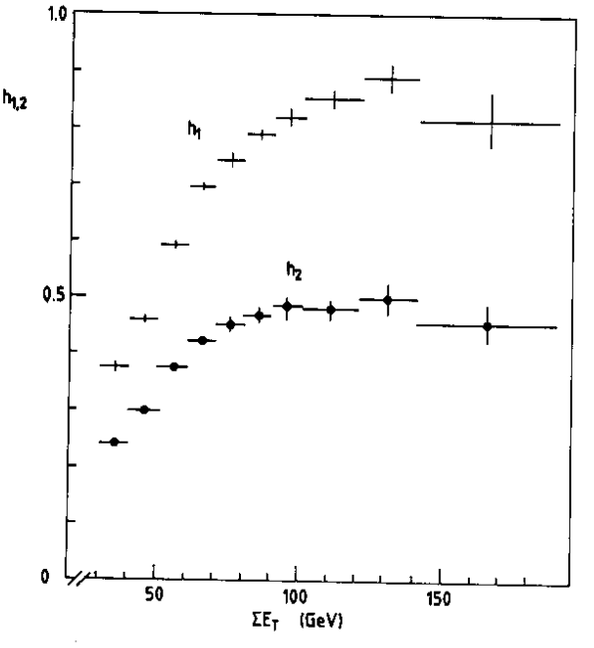

Figure 4.
Two-jet dominance : the dependence of h_1 and h_2 upon ΣE_T (see text).

3.2 - DATA REDUCTION.

The responses of the electromagnetic calorimeter to energies deposited by photons and by hadrons differ by typically 20%. In the present very preliminary analysis we ignore this fact and simply measure the energy in a cell as the sum of the energies in the three compartments (at least one compartment must have 150 MeV, well above pedestal fluctuations). We also join adjacent cells, each containing at least 400 MeV, in clusters having an energy measured as the sum of the cell energies (we split clusters having a "valley" more than 5 GeV deep). The errors resulting from these simplifications and from the fact that the dependences of the calorimeter response upon impact and energy are not taken into account are of the order of ±10%. They can be reduced to a negligible level after proper correction but only uncorrected data are presented in this Section.

A small background contamination of beam halo particles interacting in the detector survives the time of flight selection in the small angle scintillator arrays. It is easily recognised from an abnormally large energy fraction measured in the hadronic compartments and is rejected from the event sample.

3.3 - TWO-JET DOMINANCE.

Figure 3 shows the distribution of the observed events as a function of their total transverse energy, ΣE_T, measured in the central calorimeter. Seventy events have $\Sigma E_T > 100$ GeV. The increased statistical accuracy is now sufficient to evidence a departure from exponential when ΣE_T exceeeds $\sim$ 60 GeV. Figure 4 illustrates clearly that this departure corresponds to the emergence of two-jet dominance at large values of ΣE_T. It shows the dependence upon ΣE_T of h_1 and h_2, the mean values of the fractions $E_T^1/\Sigma E_T$ and $(E_T^1 + E_T^2)/\Sigma E_T$, where E_T^1 and E_T^2 are the largest and second largest transverse energies of the clusters in an event, respectively. An event containing only two jets of equal transverse energies would have $h_1 = 0.5$ and $h_2 = 1$. Immediate evidence for two-jet dominance is also obtained from a simple inspection of the energy distribution in the θ-ϕ plane : examples are shown in Figures 5a to d.

The azimuthal separation between the two clusters having the largest transverse energies ($E_T^{1\,2} > 15$ GeV) in events having $\Sigma E_T > 80$ GeV is observed to peak near 180^o (Figure 6).

In the present data (Figure 7) 400 events (compared to 3 in the 1981 data) contain a large E_T cluster (jet) having a transverse energy in excess of 40 GeV. The evaluation of the jet production cross-section from the observed distribution of jet transverse energies shown in Figure 7 implies corrections to the energy scale and evaluations of acceptance and detection efficiencies which are beyond the scope of this preliminary report.

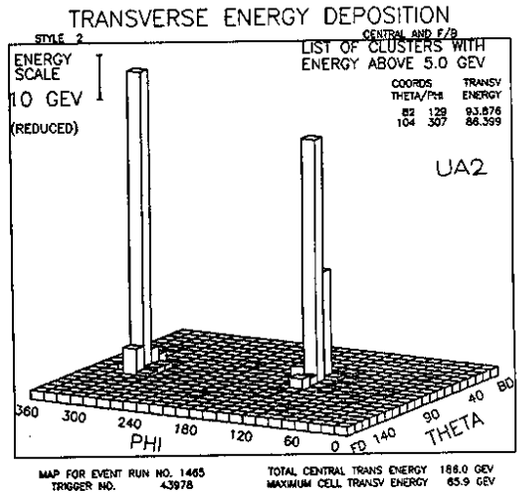

a)

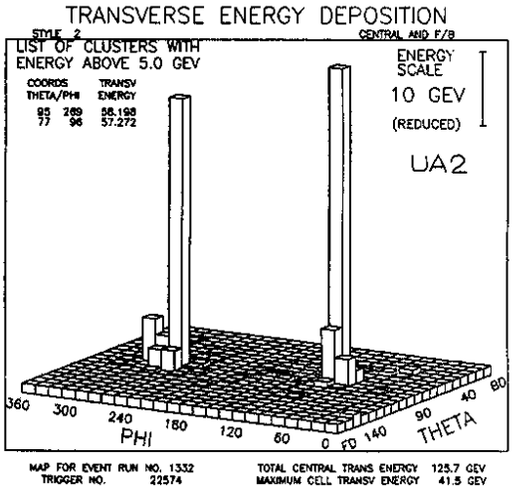

b)

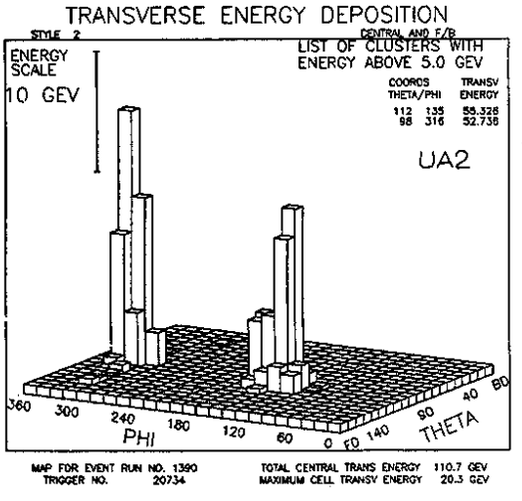

c)

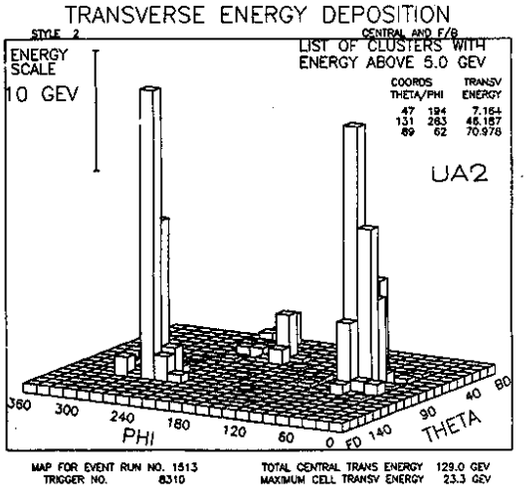

d)

Figure 5 a to d.
Typical θ-ϕ distributions of the transverse energy in large ΣE_T events.

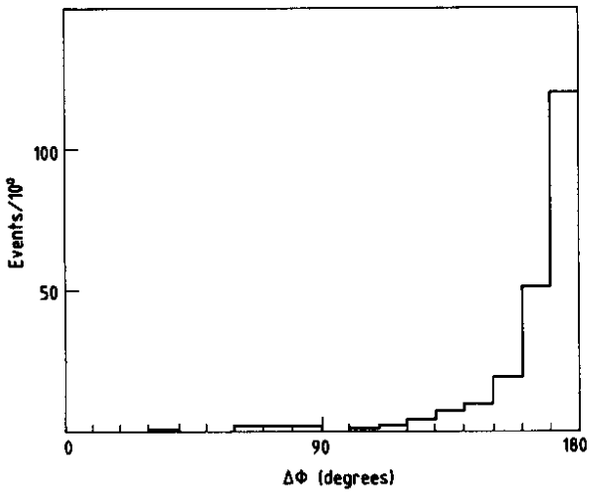

Figure 6. Azimuthal separation $\Delta\phi$ between two jets, each having $E_T > 15$ GeV, in events with $\Sigma E_T > 30$ GeV.

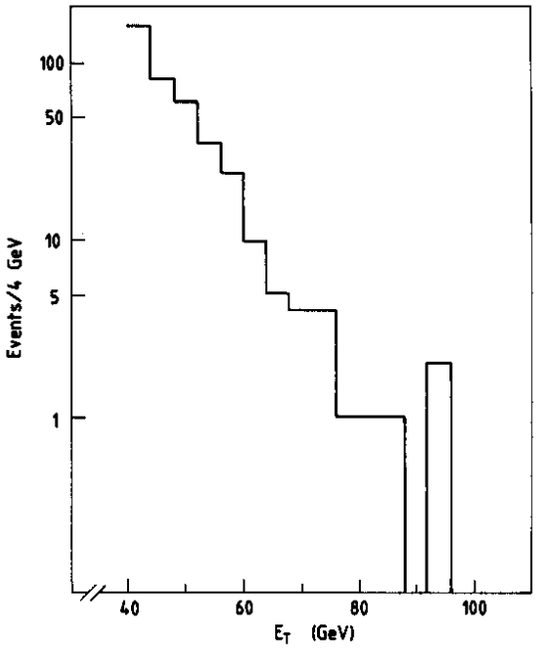

Figure 7. Observed (uncorrected) transverse energy distribution of jets having $E_T > 40$ GeV.

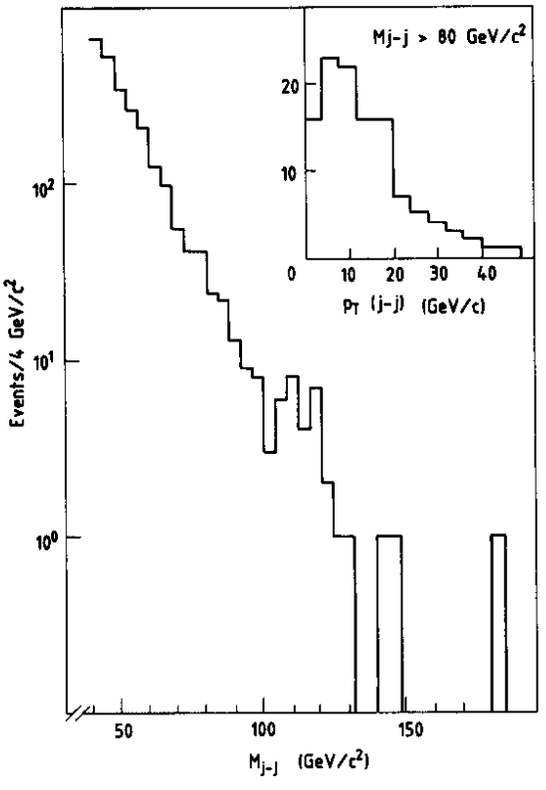

Figure 8. Two-jet invariant mass (M_{j-j}) distribution (uncorrected). The observed (uncorrected) transverse momentum distribution of two-jet systems having $M_{j-j} > 80$ GeV/c^2 is shown in the insert.

Finally we show in figure 8 the uncorrected invariant mass (M_{j-j}) distribution of the two-jet systems and their transverse momentum distribution for $M_{j-j} > 80$ GeV/c^2. While the invariant mass distribution shows no significant structure, it is not inconsistent with the presence of $\sim$ 20 events in the 80 ± 10 GeV/c^2 region from hadronic decays of the electroweak bosons. Such decays are expected to proceed mainly via $q\bar{q}$ pairs.

4. SEARCH FOR W → eν DECAYS.

The decay into $e^{\pm}\nu$ of a $W^{\pm}$ produced at rest in a $\bar{p}p$ collision would generate a monochromatic electron with energy $E^{el} = \frac{1}{2} M_W$, M_W being the rest mass of the W boson. In practice W's are expected to be produced with important longitudinal momenta. This does not affect the transverse momentum distribution of the decay electron which peaks near its end point at $E_T^{el} = \frac{1}{2} M_W$ (Jacobian peak). An interesting feature of the leptonic decay mode of the $W^{\pm}$ is the presence of parity violating terms in the angular distribution of the leptons. If the $W^{\pm}$ is produced with helicity $\varepsilon = \pm 1$, the angular distribution of the lepton (e^- for W^-, ν for W^+) is of the form $(1 - \varepsilon \cos\theta^*)^2$, where θ^* is the lepton angle in the W centre of mass with respect to the W momentum.

W's are also expected to be produced with important transverse momenta [8], similar to that of a two-jet system of a same mass (see Figure 8, where however part of the measured transverse momentum is of instrumental origin). This results mainly in a smearing of the Jacobian peak but does not induce significant correlations between the transverse momentum of the decay electron and that of the W (or of its associated recoil particles). We shall therefore search for large transverse momentum electrons which are not accompanied by other particles at small angle to the electron momentum. This simplified approach will strongly reduce a possible two-jet background and should not affect seriously the W → eν signal. However it precludes any search for large transverse momentum electrons among jet fragments.

We shall deal separately with the central and forward regions in which different experimental methods are used. In both cases the initial event sample is that of W-triggers.

4.1 - SEARCH FOR W → eν IN THE CENTRAL REGION.

We first search for energy clusters in the central calorimeter which have a configuration consistent with that expected from an isolated electron : the cluster must be contained in a 2 × 2 cell quartet of the electromagnetic calorimeter, the leakages in the associated hadronic cells and in the adjacent electromagnetic cells must not exceed 10% each. In addition we exclude clusters having

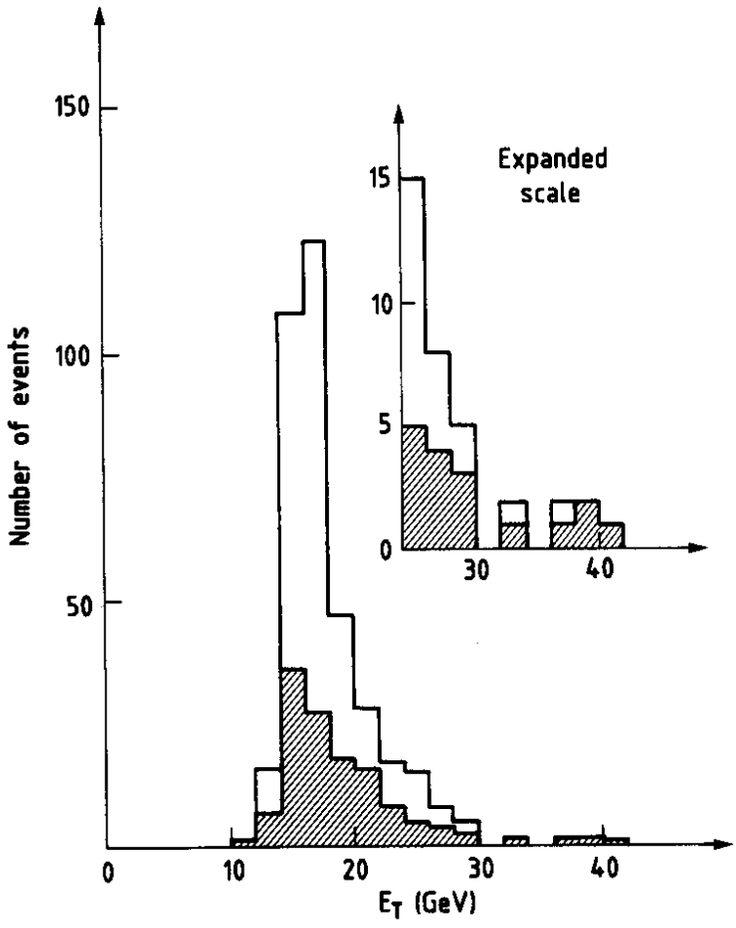

Figure 9.

Transverse energy distribution of an initial sample of 365 events from which electron candidates in the central calorimeter are selected. The cross-hatched distribution (133 events) is for events having a track pointing to the calorimeter cluster.

their centroid in a cell located at a boundary of the calorimeter acceptance. These straightforward requirements leave only 365 events in which such a cluster has a transverse energy E_T in excess of 15 GeV (including transverse and longitudinal leakages), with only seven events above E_T = 30 GeV. The E_T distribution is shown in Figure 9.

This sample is further reduced by simply requiring that at least one track measured in the vertex detector points to the energy cluster. If $\delta\theta$ and $\delta\phi$ are the angles between the track and the line joining the event vertex to the cluster centroid we require that $\delta = |(\delta\theta/10^o)^2 + (\delta\phi/15^o)^2|^{\frac{1}{2}} < 1$, a condition always satisfied by single electrons. Figure 9 shows the E_T distribution in the remaining event sample. We note that much of the reduction from 365 to 133 events occurs at low E_T values.

At this stage of the analysis, hadron jets having unusual fragmentation modes are expected to be the main background contamination. In particular narrow pairs consisting of a π^0 and a charged hadron are still to be rejected. To further enrich the sample of electron candidates we apply the following additional selection criteria :

- no other track should point to a charge cluster measured in the preshower counter. The quality of the match with the cluster measured on the proportional wires should be < ±1 cm, and with the cluster measured on the cathode strips < ±2 cm. These values are obtained from "normal events" collected with a trigger requiring a simple coincidence between the small angle scintillator arrays (Figure 10a). In the event sample presently under study the track-cluster correlation is obscured by the presence of π^0 conversions (Figure 10b).
- the charge of the preshower cluster should be at least four times larger than the most probable charge deposited by a minimum ionizing particle (Figure 11). This condition was measured (using 28 and 50 GeV electron beams) to be satisfied by electrons with a probability of $\sim$ 90%. Together with the requirement of no hadron calorimeter leakage, it rejects single charged hadrons at a level of $\sim 10^3$ (Figure 12).
- if other preshower clusters are measured within 10^o of the selected track, their total charge should not exceed 25% of the charge of the cluster to which the selected track is observed to point.

Figures 13a to c illustrate the efficiency of the preshower counter at rejecting overlap background. Note that radiative corrections to $W \to e\nu$ decays should result in $\sim$ 5% of the decay electrons being accompanied by a photon of 10 MeV or more within 10^o.

The application of the above selection criteria leaves only 9 events containing an electron candidate having E_T in excess of 15 GeV. The E_T distribution is

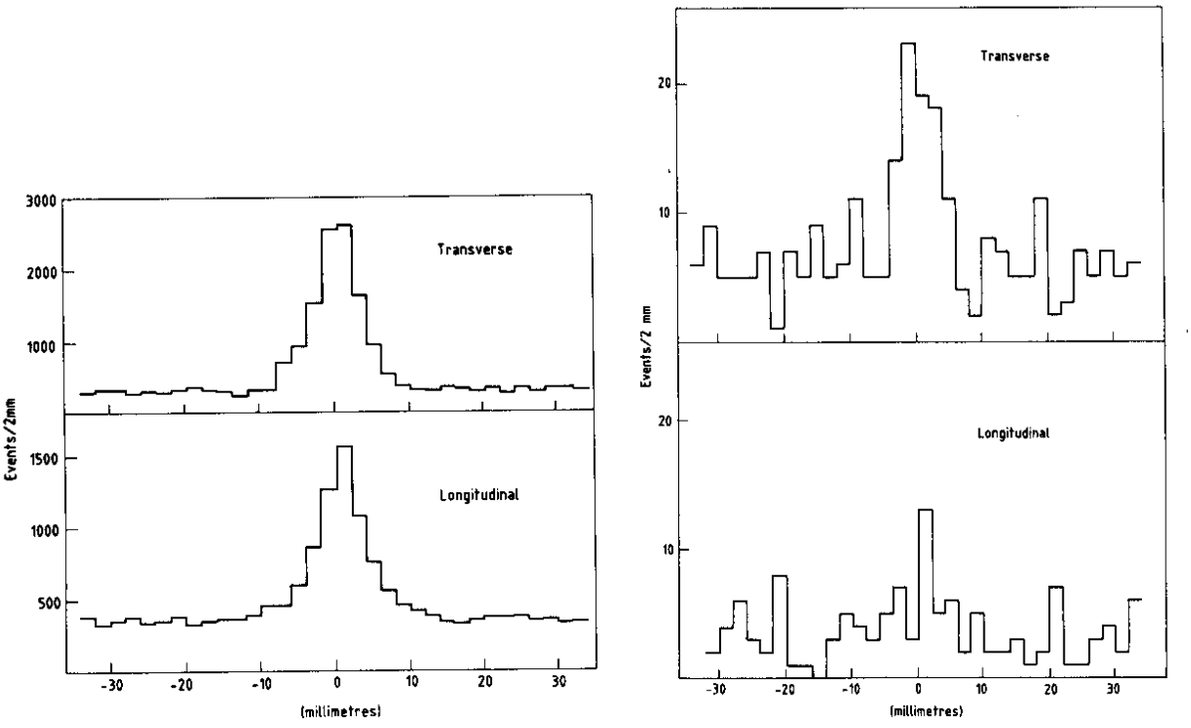

a) b)

Figure 10. Track-cluster distance in the central preshower counter in the transverse (wires) and longitudinal (strips) views
a) for minimum bias events
b) for the sample of electron candidates.

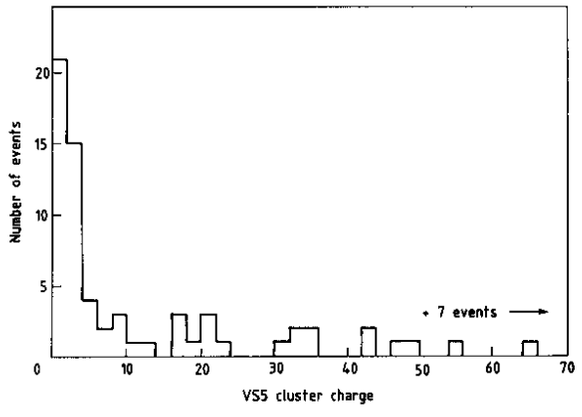

Figure 11. Charge distribution of the preshower counter (wires) for the sample of electron candidates. Charges are measured in minimum ionising particle equivalents.

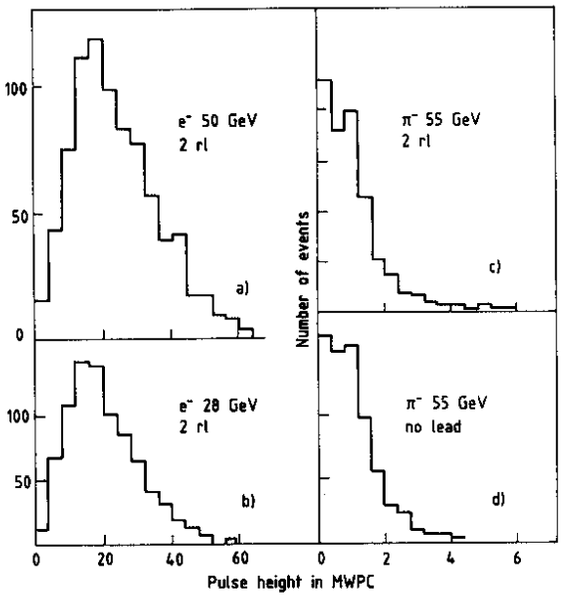

Figure 12. Pulse height distributions measured in the preshower counter using electrons and pions from a test beam. Units are minimum ionising particle equivalents.

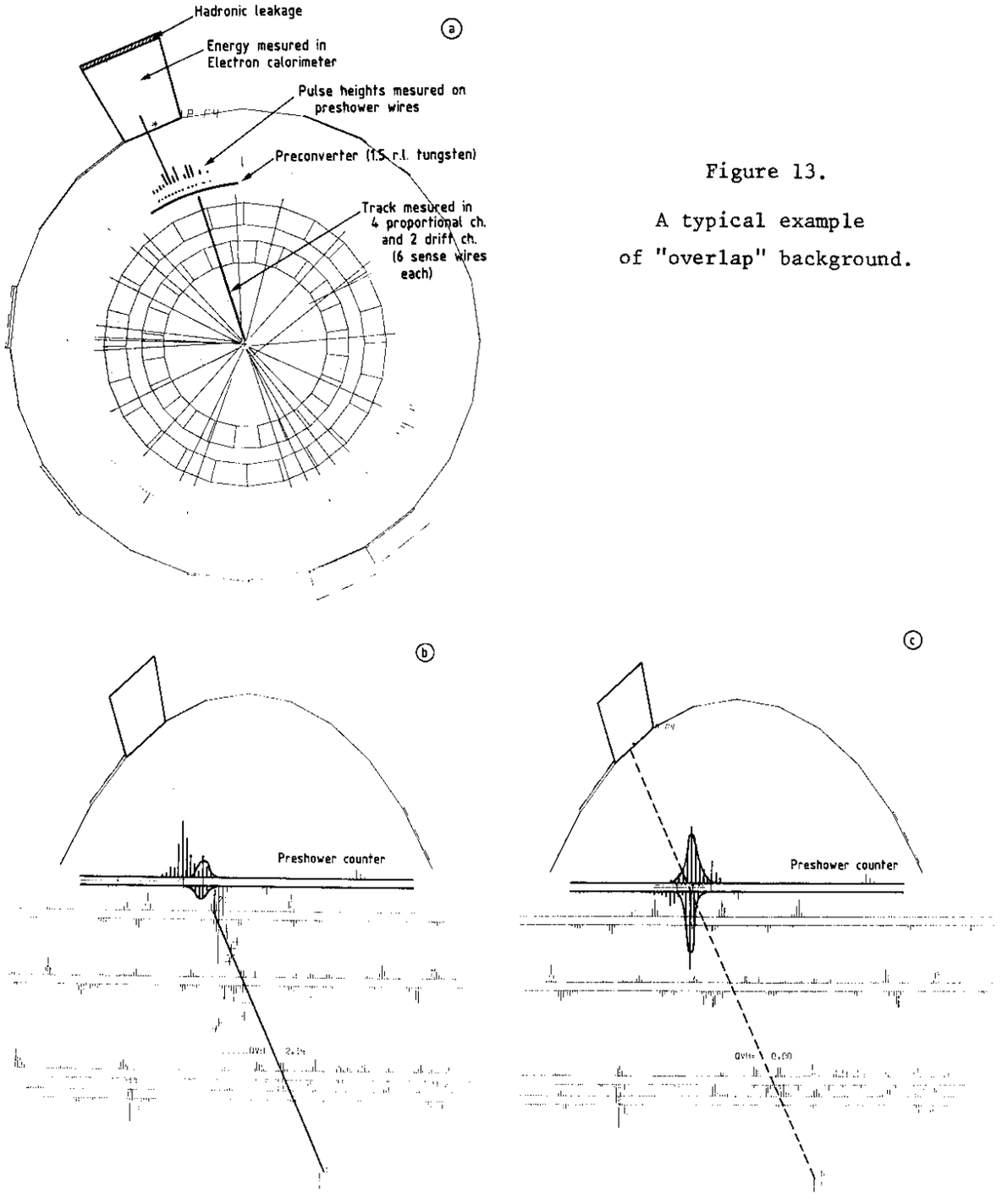

Figure 13.

A typical example
of "overlap" background.

a) transverse view : the charged track measured in the vertex detector points to the smaller preshower cluster.

b) longitudinal view in the azimuthal plane of the track. Facing strip clusters in the preshower counter have small pulse heights.

c) longitudinal view in the azimuthal plane of the larger wire cluster. Facing strip clusters in the preshower counter have large pulse heights. They are attributed to a π^0 (dotted line) having converted in the tungsten preconverter.

shown in Figure 14. It is remarkable that most of the reduction has taken place at low E_T values.

Background from standard sources are expected to contribute a negligible contamination to the remaining event sample. In particular we have observed $\sim 10^3$ jets in a 10 GeV wide band around $E_T = 30$ GeV (Figure 7). At a same value of E_T we expect to have $\lesssim 10$ single hadrons since the ratio between jet and hadron inclusive production cross sections is $\lesssim 10^2$ [2]. The rejection against charged hadrons provided by the detector is $\sim 10^3$ corresponding to a background contamination of only $\sim 10^{-2}$ event. Similarly the contribution of photon conversions in the vacuum pipe or of internal Dalitz conversions can only amount to $\sim 3\%$ per photon. If they were dominant in the final sample many more unconverted photons should have been found (as long as they do not belong to very high multiplicity photon clusters). This is contrary to the observation that of 7 clusters with $E_T > 30$ GeV only 2 were not associated with a track. More work is however needed to ensure that we did not overlook other possible background sources and to further ascertain electron identification.

For $W \to e\nu$ decays, the non observation of the decay neutrino should result in an apparent transverse momentum imbalance. To study this effect we evaluate the total transverse momentum carried by particles detected within the whole UA2 acceptance, P_T^{tot}. This evaluation accounts for particles detected in the wedge and forward spectrometers. The fraction

$$f = |\vec{P}_T^{tot}| \; / \; E_T^{el}$$

should near 1 for actual W decays and take smaller values in events without balancing neutrino - to the extent that the detector coverage is sufficient to catch most of the transverse energy produced in the collision.

The distribution of f in the sample of the nine retained events is shown in Figure 15. The events with the larger f values ($f > 0.6$) are indicated on Figure 14. It is remarkable that they are also the events having the larger E_T^{el} values. Figure 16 illustrates the ability of the UA2 detector to measure the transverse momentum imbalance on hadron jets selected from the W trigger sample by requiring a hadronic leakage exceeding 25%. The nine events of the final sample are shown on the same plot.

The energy distribution in the θ-ϕ plane of one of the three imbalanced events is shown in Figure 17 and the corresponding electron track in Figure 18. In all three events there is very little transverse energy observed beside that of the large transverse momentum electron candidate.

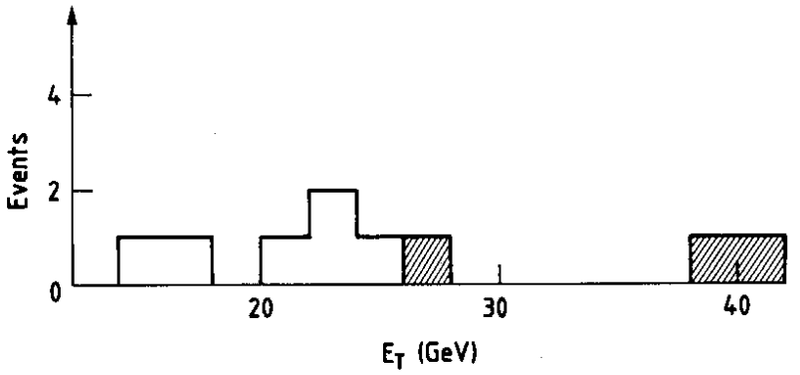

Figure 14. Transverse energy distribution of the 9 electron candidates having $E_T > 15$ GeV. The three cross-hatched events satisfy the cut $f > 0.6$ (see Figure 15).

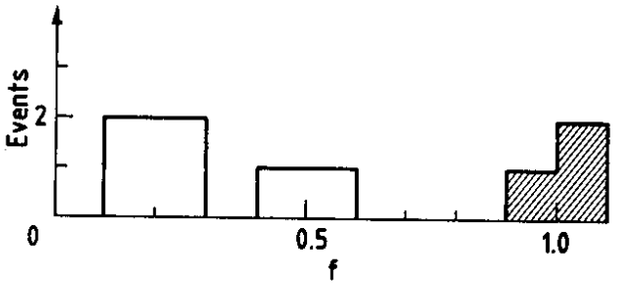

Figure 15. Transverse energy imbalance for the central calorimeter electron candidates (see text).

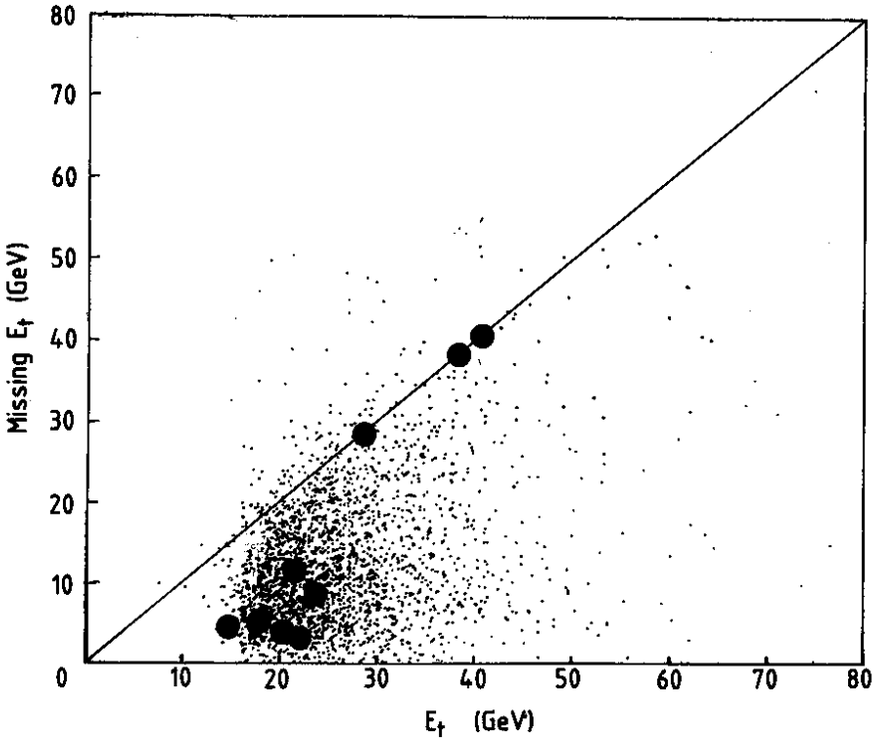

Figure 16. The nine electron candidates (black circles) are compared with two-jet events (dots) in the "transverse energy" versus "imbalance" plane (see text).

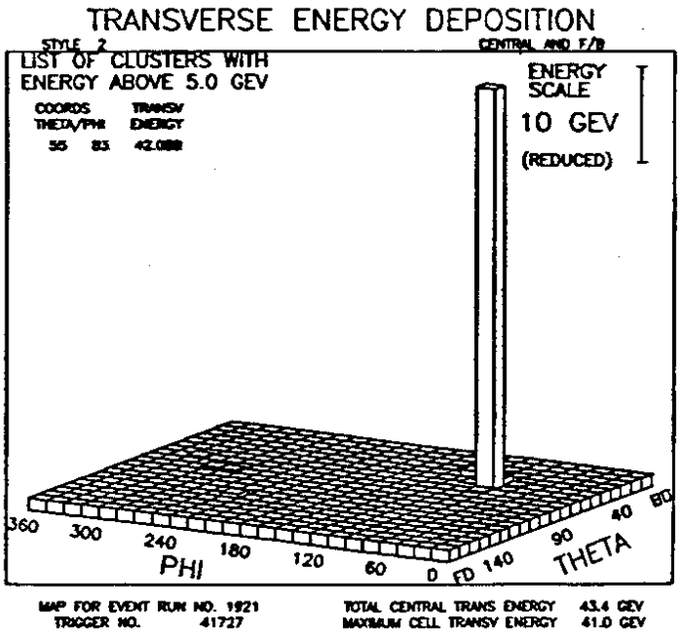

Figure 17. Transverse energy distribution of one of the imbalanced electron candidates in the θ-ϕ plane.

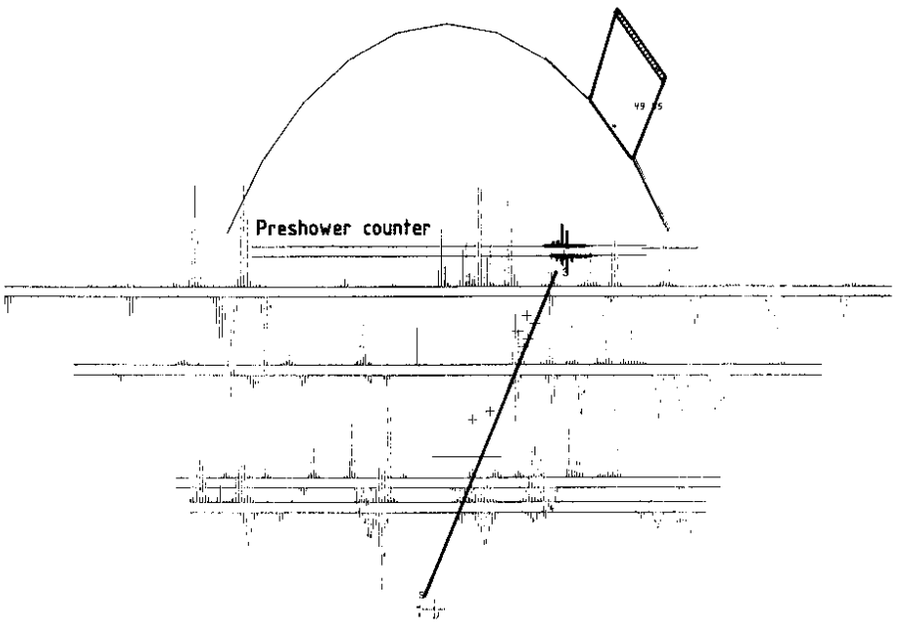

Figure 18. Longitudinal view of the electron track for one of the imbalanced candidates.

4.2 - SEARCH FOR $W \to e\nu$ IN THE FORWARD REGIONS.

The search for $W \to e\nu$ decays in the forward regions follows the same general guidelines as in the central region.

Each of the two forward detectors covers a range of scattering angles $20^\circ < \theta < 37.5^\circ$ and is instrumented in 12 azimuthal sectors ($\Delta \phi \sim 30^\circ$) with magnetic spectometers (Figure 19). The magnetic fields are generated from two "lamp-shade" magnets of 12 coils each. The field integral is 0.38 Tm on the average and the loss of azimuthal coverage caused by the magnet coils is $\sim$ 18%.

Depending on the sign of their charge, particles are bent towards or away from the beam line and their deflected tracks are measured in three triplets of drift chambers. Each triplet is made of chambers having sense wires at -7°, 0° and $+7^\circ$ to the magnetic field direction. In the present preliminary analysis the resolution achieved in momentum measurement is $\Delta(\frac{1}{p}) \simeq 2\%\ GeV^{-1}$. This value will be substantially improved in the future. Each magnetic spectrometer sector is followed by a preshower counter and an electromagnetic calorimeter. The preshower counter consists of a 1.4 radiation length thick lead converter preceding two proportional tube chambers. Each electromagnetic calorimeter sector is subdivided in 10 cells, each covering a rapidity $\times$ azimuth domain $\Delta y \times \Delta\phi \simeq 0.17 \times 15^\circ$ similar to that covered by the central calorimeter cells. Each cell is segmented in two compartments, one 24 radiation length thick in which most of electromagnetic showers are contained, the other 6 radiation length thick serving as a veto against hadronic showers. The response and performance of the preshower counters and calorimeters have been extensively studied in a 10 GeV electron beam. In particular the dependence of the calorimeter response upon impact point in each cell has been accurately measured. A comparison of the two phototube signals receiving light from the wave-shifting light guides on each side of a cell allows to localise the impact point to within ± 2 cm.

The following selection criteria are applied to the sample of W triggers to select possible electron candidates :

- a transverse energy deposition exceeding 10 GeV must be measured in one of the forward sectors. It must be associated with a track measured in the corresponding spectrometer and, depending upon the position of the track impact, it must be contained in one or at most two cells.
- leakage in the veto compartment must not exceed 2%, a condition satisfied by $\sim$ 98% of 40 GeV electrons (Figure 20).
- the proportional tubes associated with the selected track must give signals. The quality of the matching between the track, the preshower counter cluster and the energy deposition in the calorimeter must fulfill selection criteria illustrated in Figures 21a to c.

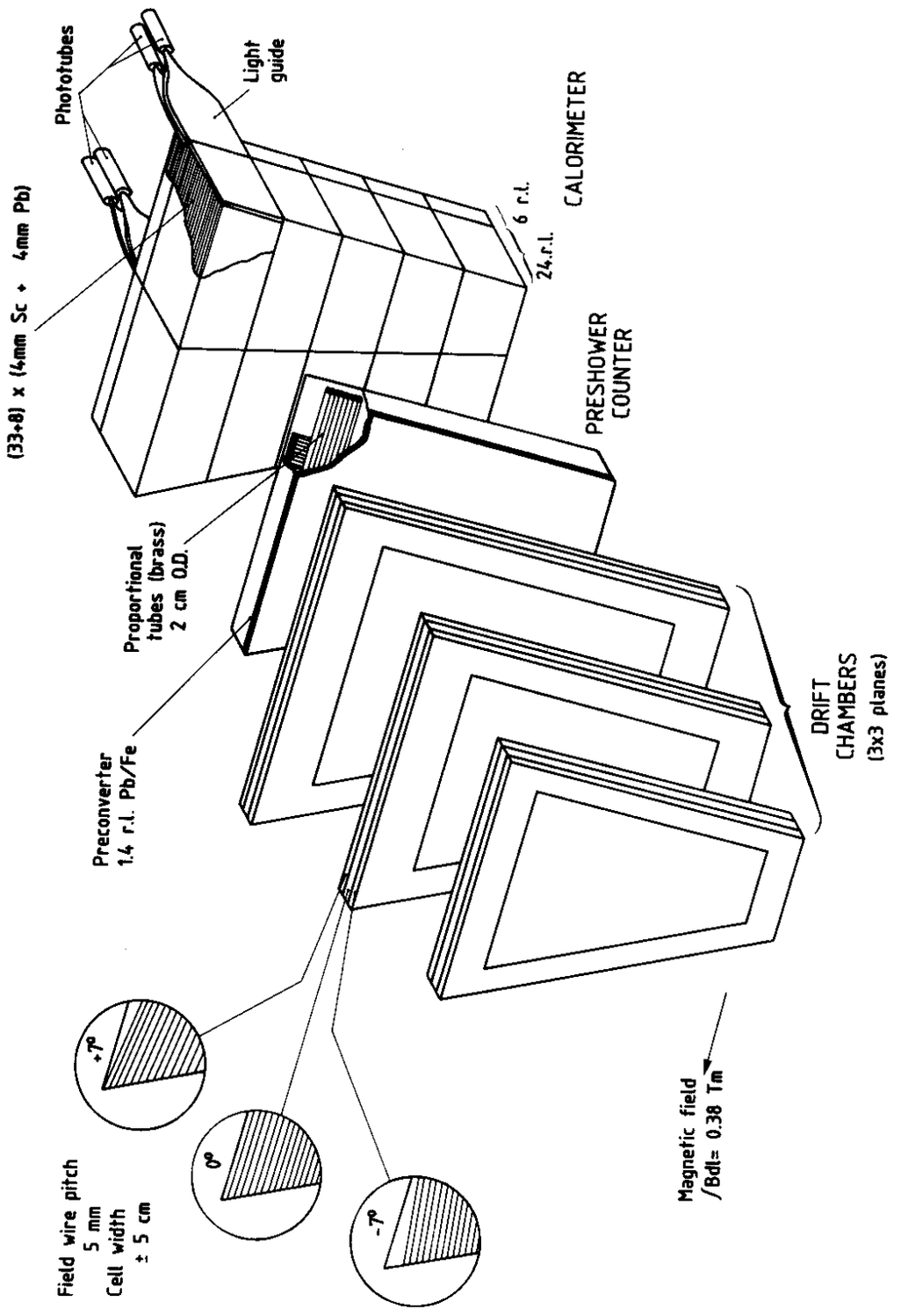

Figure 19. Schematic view of one of the 24 sectors of the forward detectors.

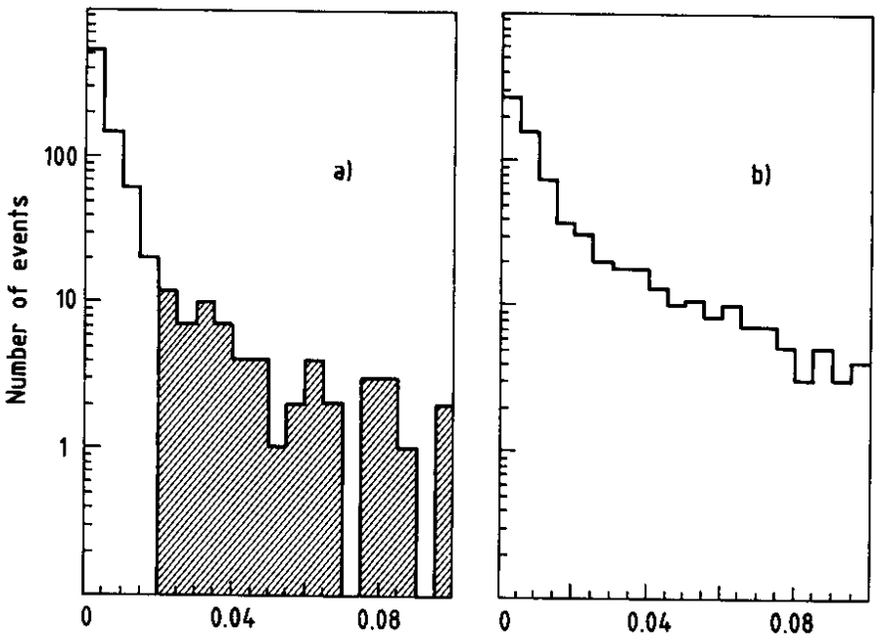

Figure 20. Leakage into the hadron veto compartment of the forward calorimeters
a) for events associated with a signal in the preshower counter,
b) for events not associated with a signal in the preshower counter.
The cut used in the analysis rejects events in the cross-hatched region.

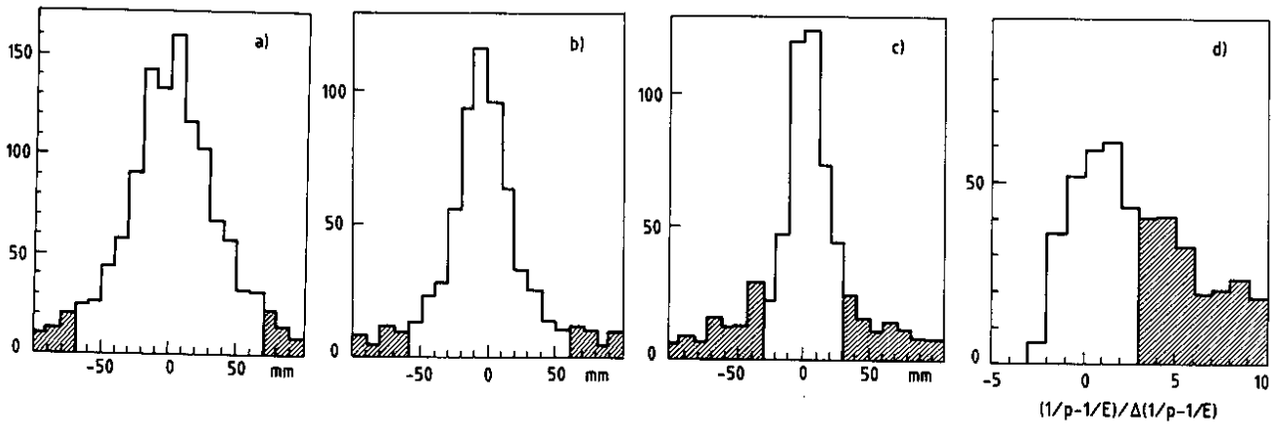

Figure 21. Matching quality criteria.
a) between the position in the calorimeter (measured from phototube ratio) and the preshower cluster (measured along the magnetic field),
b,c) between the track measured in the drift chambers and the preshower cluster (measured along the magnetic field and normal to it respectively)
d) between the momentum measurement in the drift chambers and the energy measured in the calorimeter for events having E_T > 10 GeV.

- the momentum p measured in the magnetic spectometer must be consistent with the energy E measured in the calorimeter. Specifically we require $\frac{1}{p}$ and $\frac{1}{E}$ to be equal within three standard deviations (Figure 21d).
- in addition to the above selection criteria we require that the electron candidate is isolated : the energy measured in adjacent calorimeter cells (including the contribution of track momenta) must not exceed 3 GeV, no other track must point to the same cell as the electron candidate and no other signal facing this cell must be measured in the preshower counter.

Ten events are found to survive these straightforward selection criteria for an integrated luminosity of $\sim$ 16 nb^{-1} (the magnets were turned off during part of the running period). The corresponding E_T distribution is shown in Figure 22.

In order to detect a possible transverse momentum imbalance we evaluate the quantity

$$f' = \vec{P}_t^{tot} \cdot \hat{e}_T / E_T^{el} ,$$

where $\hat{e}_T$ is the unit vector directed along the transverse momentum of the electron candidate. The f' distribution in the remaining sample of 10 events is shown in Figure 23 and the four events having f' > 0.6 are indicated in Figure 22. It is remarkable that the event with the largest E_T^{el} value survives this cut. Some features of this event are illustrated in Figures 24 and 25.

4.3 - CONCLUSION.

The application of rather straightforward selection criteria has reduced the original sample of W-trigger events to a level of only 9 events in the central region and 4 events in the forward regions containing an electron candidate having E_T > 15 GeV.

We have scanned visually a large number of events containing an electron candidate, in particular the 365 events of the originally selected sample in the central region. The scan has confirmed the results of the analyses presented in the preceding sections.

It is remarkable that the four events containing an electron candidate having E_T > 15 GeV and a strong transverse momentum imbalance have an E_T distribution which is consistent with that expected for $W \to e\nu$ decays. More over their rate of occurence is also in excellent agreement with current expectations.

The nine events in which the transverse momentum of the candidate electron is partly balanced by other hadrons detected in the UA2 apparatus often contain a clear jet at opposite azimuth to the electron candidate. While background from obvious sources (conversions, misidentified single hadrons) are expected to be small more work is needed to ensure that possible unexpected backgrounds have not been overlooked and to further ascertain electron identification.

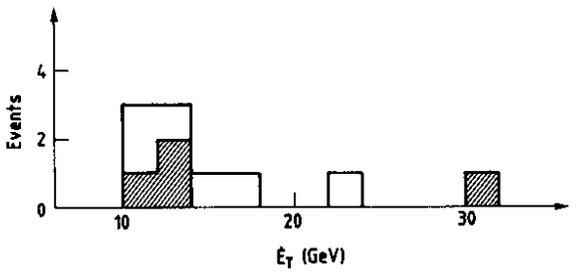

Figure 22. Transverse energy distribution for the ten electron candidates in the forward detectors. The four cross-hatched events are imbalanced ($f' > 0.6$).

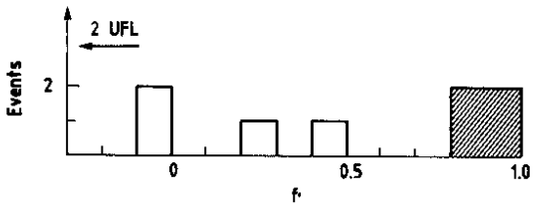

Figure 23. Transverse energy imbalance for the forward detector electron candidates (see text).

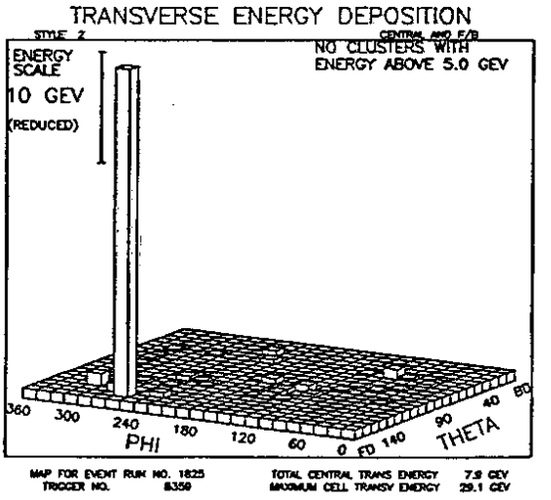

Figure 24. Transverse energy distribution of the imbalanced electron candidate having E_T = 3 GeV in the θ-ϕ plane.

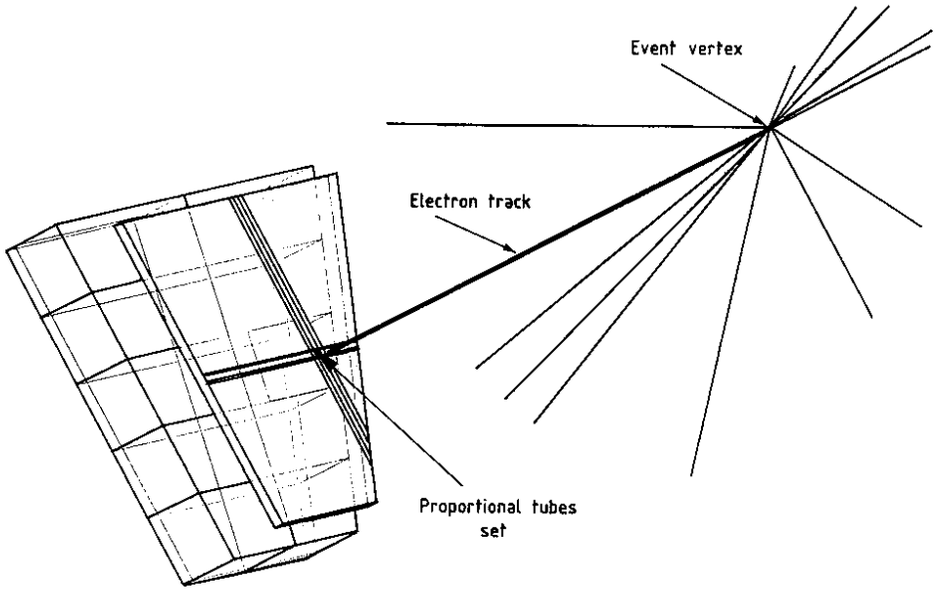

Figure 25. Perspective view of the event having an electron candidate with E_T = 30 GeV in the forward detector.

5. SEARCH FOR $Z^0 \to e^+e^-$ decays.

A search for electron pairs having an invariant mass in excess of 40 GeV/c^2 has been conducted by selecting events of the Z-trigger sample in which two quartets of electromagnetic cells (central and forward regions were considered together) were found to have transverse energies E_T^1 and E_T^2 such that $E_T^1 + E_T^2 > 30$ GeV.

Although the Z-trigger did not require a coincidence with the small angle scintillator arrays, all events of the selected sample in which this coincidence was not satisfied have been observed to result from sources other than $\bar{p}$-p collisions (cosmic rays, beam halo, etc...).

Of the 257 events selected, none survived very simple selection criteria. All were scanned visually and most of them show typical two-jet configurations.

ACKNOWLEDGEMENTS

We gratefully acknowledge the remarkable performance of the Staff of the $\bar{p}p$ project and of the operation crews of the relevant CERN accelerators. We thank the UA4 Collaboration who let us use their small angle scintillator hodoscopes.

We are deeply indebted to the technical staffs of the Institutes Collaborating in UA2. Financial support from the Danish Natural Science Research Council to the Niels Bohr Institute group and from the Schweizerischer National fonds zur Förderung der wissenschaftlichen Forschung to the Bern group are acknowledged.

REFERENCES

[1] The Staff of the CERN proton-antiproton project, Phys. Lett. 107B (1981) 306.

[2] M. Banner et al., Phys. Lett. 118B (1982) 203.

[3] M. Banner et al., Phys. Lett. 115B (1982) 59.
M. Banner et al., Phys. Lett. 121B (1983) 187.
M. Banner et al., Inclusive charged particle production at the CERN $\bar{p}p$ Collider, to be published in Phys. Lett.

[4] S. Weinberg, Phys. Rev. Lett. 19 (1967) 1264.
A. Salam, Proc. 8th Nobel Symposium, Aspenäsgården, 1968 (Almqvist and Wiksell, Stockholm, 1968), p. 367.

[5] See for example C. Quigg, Rev. Mod. Phys. 94 (1977) 297.

[6] A.G. Clark, Proceedings of the Int. Conf. on Inst. for Colliding Beam Phys., SLAC, 1982.
The UA2 Collaboration, First results from the UA2 experiment, presented at the 2nd Int. Conf. on Physics in Collisions, Stockholm, Sweden, 2-4 June 1982.

[7] R. Battiston et al, Phys. Lett. 117b (1982) 126.

[8] F. Halzen and D.M. Scott, Phys. Lett. 78B (1978) 318.
P. Aurenche and F. Lindfors, Nucl. Phys. b185 (1981) 301.
F. Halzen, A.D. Martin, D.M. Scott and M. Dechantsreiter, Phys. Lett. 106B (1981) 147.
M. Chaichian, M. Hayashi and K. Yamagishi, Phys. Rev. D25 (1982) 130.
F. Halzen, A.D. Martin and D.M. Scott, Phys. Rev. D25 (1982) 754.
V. Barger and R.J.N. Phillips, University of Wisconsin preprint MAP/PH/78 (1982).
W.L. van Neerven, J.A.M. Vermaseren and K.J.F. Gaemers, NIKHEF preprint NIKHEF-H/82-20 (1982).